XLIII
CILAMCE
21-25, November, 2022
FOZ DO IGUAÇU - PR - BRAZIL

NUMERICAL SIMULATION OF THERMOCAPILLARY FLOW 2D AND 3D: A BI-PHASE SMOOTHED PARTICLE HYDRODYNAMICS APPROACH

E. A. Patiño-Nariño[1], A. F. Galvis[2], R. Pavanello[3], M. R. Gongora-Rubio[1]

[1]*Micromanufacturing Laboratory, Bionanomanufacturing Center, Institute for Technological Research of the São Paulo State*
Avenida Professor Almeida Prado, 05508-901, São Paulo/SP, Brazil
edgarandres@ipt.br, gongoram@ipt.br
[2]*School of Mathematics and Physics, University of Portsmouth*
Winston Churchill Avenue, PO1 2UP, Portsmouth, UK
andres.galvis@port.ac.uk
[3]*Department of Computational Mechanics, School of Mechanical Engineering, University of Campinas*
Rua Mendeleyev, 13083-860, Campinas/SP, Brazil
pava@fem.unicamp.br

Abstract. This work presents a Smoothed Particle Hydrodynamics (SPH) method for modeling the heat transfers, natural convection, and thermal Marangoni effects at the interface with density variation and bi-phase fluid flows in two and three dimensions. A capillary interface (surface tension) scheme was implemented with the Continuum Surface Force (CSF) model and the approximation of the SPH to the Navier-Stokes equations for delimiting stable interfaces and smooth bi-phase to allow the simulation of flows between liquid-liquid and liquid-gas. Moreover, the solution strategy with SPH for the combination of temperature gradient (heat transfers), gravity, and surface tension, as required for modeling the Marangoni forces, is verified with related cases of study. Problems of thermally driven flow and Bernard convection in cavities are studied to validate the heat transfer and convection. The solutions are displayed in respect of temperature, velocity fields, and Nusselt number, with different Rayleigh numbers (Ra) regimes ($10^3 \leq \text{Ra} \leq 10^6$). Thus, the bi-phase method applies the thermo-capillary flow, in the migration rises a droplet due to a surrounding fluid with a linear temperature gradient. In these cases, different aspects of the dynamics of the thermo-capillary flow were considered for verification. Finally, the numerical examples show that the SPH and CSF proposal is efficient, reliable, and with good precision in modeling inter-facial flow problems under hydrodynamic and thermal influences.

Keywords: Thermo-capillarity, Bi-phase flow, Smoothed Particle Hydrodynamics.

1 Introduction

Multiphase interfaces in fluids are often unstable with the presence of heat transferred. These instabilities generally occur during the flow of migration fluids due to heat, capillarity, and phase recombination [1]. Currently, a simulation of these cases has interested the attention of both the academic and industrial communities. However, situations in domains with density ratios, heat transfer, and capillarity interacting with the fluid flow are complex and difficult to predict and model [2].

A mesh-free method with Lagrangian formalism and successful simulations of problems with multiphase interaction is the SPH method [3]. The SPH method seems well suited for multi-fluid flow interface problems in presence of the thermal influence. However, the implementation of 3D SPH for multiphase flows is recent, and still requires adequate validations, especially in cases with surface tension, density ratios and their influence with temperature and external body forces (gravity). Currently, the fluid simulation with SPH uses the Navier-Stokes equations, associated with the CSF method and Boussinesq approximation [4]. This approach has been well-test for the implementation of capillary and heat transference phenomena for fluid-fluid and fluid structure [3]. Thus, the SPH method has lately been used for multiphase flow problems, reaching promising in applications of the thermo-capillary and natural convection problems [4, 5].

Migration of a droplet in 2D and 3D in the conditions of the thermo-capillary flow over the droplets is explored.

The drop moves due to surface tension gradients tangential to the interface that occurred by a temperature gradient migration (even without the influence of gravity). For high low Reynolds numbers (laminar regimes), the droplet morphology is kept constant circular/spherical during the motion [11].
Therefore, the present work aims to propose and develop a consistent SPH method that is capable of dealing with complex flow physics, including heat exchange, Marangoni forces, and thermo-capillary effects. The fundamental contribution of this study is the implementation of an effective density-independent formulation based on a 3D classical weakly compressible bi-fluid SPH. Finally, the proposed SPH is a promising methodology for problems of thermally driven flow (square and Bernard natural convection) and the thermo-capillary flow in the upward migration of the droplet due to a surrounding fluid with a linear temperature gradient.

2 SPH formulation of bi-phase model

It is important to reformulate the density-independent SPH method for the multi-phase conditions [6]. Thereby, the evolution of density is formulated, as follows:

$$\left\langle \frac{d\rho}{dt} \right\rangle_i = \rho_i \sum_{j=1}^{N} V_j \left(\mathbf{v}_{ij}\right) \cdot \nabla_i W_{ij} \quad \text{and} \quad V_i = \left(\sum_{j=1}^{N} W_{ij} \right)^{-1} \quad , \tag{1}$$

where ρ_i and V_i denotes density and volume in the ith particle, respectively. ∇_i is the derivative with respect to its position $\mathbf{r}_i$, $\mathbf{v}_{ij} = \mathbf{v}_i - \mathbf{v}_j$ is the relative velocity between the ith and jth particles, N is particle number and W_{ij} represents the quintic spline kernel function [3]. The dynamic viscous coefficient, pressure and volume should be modified to an inter-particle average [7] approximation form

$$\tilde{\mu}_{ij} = \frac{2\mu_j \mu_i}{\mu_j + \mu_i} \quad , \quad \tilde{P}_{ij} = \frac{(P_i \rho_j + P_j \rho_i)}{\rho_i + \rho_j} \quad \tilde{\kappa}_{ij} = \frac{2\kappa_j \kappa_i}{\kappa_j + \kappa_i} \quad \text{and} \quad \tilde{V}_{ij} = \left(V_i^2 + V_j^2\right) \quad . \tag{2}$$

Thus, the weakly compressible fluid of the momentum written in the Lagrangian reference frame is approximated as:

$$\left\langle \frac{d\mathbf{v}}{dt} \right\rangle_i = \frac{1}{m_i} \sum_{j=1}^{N} \left[-\left(\tilde{P}_{ij} + P_0\right) + (2 + \mathrm{d})\tilde{\mu}_{ij} \frac{\mathbf{r}_{ij} \cdot (\mathbf{v}_i - \mathbf{v}_j)}{r_{ij}^2 + \varepsilon^2} \right] \tilde{V}_{ij} \nabla_i W_{ij} + \frac{\mathbf{f}^{(st)}}{\rho_i} + \Theta_i + \mathbf{g} \quad , \tag{3}$$

where P, μ, $\mathbf{g}$, d, and h are the fluid pressure, the kinetic viscosity, the body force vector (the gravity force), spatial dimension (2 or 3), and the smooth kernel length, respectively. Also, $\mathbf{r}_{ij} = \mathbf{r}_i - \mathbf{r}_j$, and $\varepsilon = 0.01h$. Furthermore, the SPH bi-phase is characterized by implementation of the interface sharpness force Θ_i [6], and CSF method for the multi-phases surface tension force term $\mathbf{f}^{(st)}$. Equation (3) is used for incompressible fluids with a low Reynolds [8], and the equation of state for compute the pressure is equal to

$$P_i = P_0 \left[(\Delta\rho_i)^7 - 1 \right] \quad , \quad \Delta\rho_i = \max \left[\frac{\rho_i}{\rho_{0,i}} \; ; \; 0.98 \right] \quad \text{and} \quad P_0 = \frac{\rho_0 c^2}{7} \quad . \tag{4}$$

Likewise, the internal energy equation is implemented for heat transfer defined as:

$$\left\langle c_p \frac{dT}{dt} \right\rangle_i = \frac{1}{\rho} \nabla \left(\kappa \nabla T\right) = \frac{1}{m_i} \sum_{j=1}^{N} \tilde{\kappa}_{ij} \left(T_i - T_j\right) \tilde{V}_{ij} \frac{\mathbf{r}_{ij} \cdot \nabla_i W_{ij}}{r_{ij}^2 + \varepsilon^2} \quad , \tag{5}$$

where T, c_p,κ, and ρ_0 are temperature, specific heat, thermal conduction, and initial fluid density, respectively.

2.1 Approximation of the $\mathbf{f}^{(st)}$ using CSF

This work uses the CSF method [9], for cases with immiscible fluids and constant surface tension. Whereby, the CSF formulation using $\mathbf{f}^{(st)}$ term in the Eq. 3 can be defined as [3]:

$$\left\langle \mathbf{f}^{(st)} \right\rangle_i = \sigma \left\langle \nabla \cdot \hat{\mathbf{n}} \right\rangle_i \left\langle \nabla C \right\rangle_i \quad , \tag{6}$$

where C is a scalar function of unit magnitude, which is expressed as

$$C_i^j = \begin{cases} 1, & \text{If} \quad i \text{ and } j \text{ particles belong to different phase } (i \neq j) \quad , \\ 0, & \text{If} \quad i \text{ and } j \text{ particles belong to the same phase } (i = j) \quad . \end{cases} \tag{7}$$

For Eq. 7, the type of phase of each particle is constant through the calculations. Thus, ∇C and $\hat{\mathbf{n}}$ are given by

$$\langle \nabla C \rangle_i = \frac{1}{V_i} \sum_{j=1}^{N} \tilde{V}_{ij} \left(\frac{C_i^j \rho_i}{\rho_i + \rho_j} \right) \nabla_i W_{ij} \quad \text{and} \quad \hat{\mathbf{n}}_i = \frac{\langle \nabla C \rangle_i}{| \langle \nabla C \rangle_i |} \quad . \tag{8}$$

Thereby, $\nabla \cdot \hat{\mathbf{n}}$ is expressed as

$$\langle \nabla \cdot \hat{\mathbf{n}} \rangle_i = \begin{cases} d \dfrac{\sum_{j=1}^{N} \left(\hat{\mathbf{n}}_i - \lambda_i^j \hat{\mathbf{n}}_j \right) \cdot \nabla_i W_{ij} V_j}{\sum_{j=1}^{N} |\mathbf{r}_{ij} \cdot \nabla_i W_{ij}| V_j}, & \text{If} \quad \min \left[| \langle \nabla C \rangle_i |; | \langle \nabla C \rangle_j | \right] > \varepsilon^2 \quad , \\ 0, & \text{otherwise} \quad . \end{cases} \tag{9}$$

being d is the spatial dimension and λ_i^j is added

$$\lambda_i^j = \begin{cases} -1, & \text{If} \quad i \text{ and } j \text{ particles belong to different phase} \quad , \\ 1, & \text{If} \quad i \text{ and } j \text{ particles belong to the same phase} \quad . \end{cases} \tag{10}$$

This coefficient introduced by A. Zhang et al. [10] is employed to reverse the direction of $\hat{\mathbf{n}}_i$, when the *i*th and *j*th particles belong to different phases.

2.2 Natural convection and thermocapillary implementations

For small density variations the Boussinesq approximation [23] is valid and the system can be considered incompressible since the pressure is still independent of the density [23]. Therefore, to include the effects of natural convection and thermo-capillary in Eqs. 3 and 6, modify the temperature change function, and external force term for the gravity constant ($\mathbf{g} = -g\hat{e}_y$) [1, 2], and the surface tension coefficient (σ), which are defined like:

$$\sigma = \sigma_0 + \sigma_T (T - T_0) \quad \text{and} \quad g = -\beta g_0 (T - T_0) \quad , \tag{11}$$

where T_0, $\mathbf{g}_0$, σ_0 are the initial conditions of temperature, external force and surface tension, respectively. However, β and σ_T are coefficients of thermal expansion and thermal dependence of surface tension (coefficient that defines the Marangoni interfacial tangential force) [11, 12]. Therefore, for all cases of this work, the hot and cold wall conditions, temperatures are configured such as $T_h = 1.0$ and $T_c = 0.0$, respectively, to define a temperature gradient of $\Delta T = 1.0$.

3 Implementation

The formulation of the time step is chosen to satisfy the Courant-Friedrichs-Lewy (CFL) conditions. Consequently, the presented formulation of the SPH is integrated over time using a predictor-corrector scheme. The particles discrete domain is built for a Cartesian distribution with particle distance Δx, and the smoothed length defined as $h = 4\Delta x/3$. This distribution is realized with the GMSH software [13]. The boundary wall conditions applying are defined through dummy particle methodology [3, 14].

The SPH code is programming using C++ and the Compute Unified Device Architecture (CUDA) developed by Nvidia to run on a Graphical Processing Unit (GPU). The code generates output data in VTK format for visualization and post-processing using the open-source data analysis software Paraview. Hence, through the Paraview visualization [15], this study incorporated the post-processing tool of streamlines of the velocity field to visualize the fluid flow, which is a traditional approach in computational fluid mechanics [16].

4 Results and Discussion

The implementations in the simulator of the Eqs. 5 and 11 of heat transfer and thermo-capillary were validated, initially for 2D. Thus, two cases to analyze the patterns of natural convection for different Rayleigh numbers (Ra) were implemented for square (Fig. 1 (a)) and rectangular (Fig. 1 (b)) cavities, for 1x1 and 1x5 domains, respectively. The rectangular case is known as the Bénard convection problem [2, 18]. For natural convection for both cases the dimensionless numbers are the Prandtl (Pr$= c_p\mu\rho/\kappa = 0.71$), and the $\mathrm{Ra} = g\beta \mathrm{L}^3\Delta\mathrm{T}/\left(\mu\kappa\right)$, where $\mathrm{L} = 1.0$ is the height of the cavity, $\beta = 1.437$, $c_p = 1.0$, $T_0 = 0.5$, $\mu = 10^{-2}$ and $\rho = 1000$.

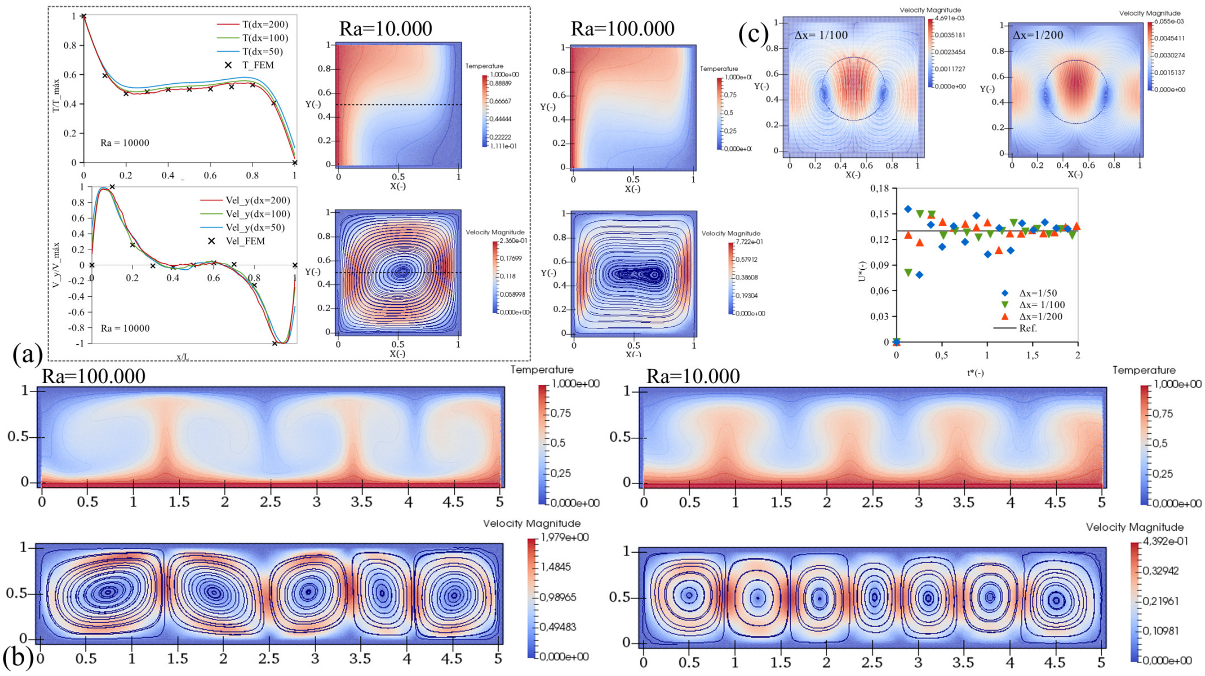

Figure 1. 2D SPH validation and calibration problems for heat exchange and thermo-capillarity: (a) Natural convection in a square cavity and the comparison of the time history with the reference solution (T_FEM and Vel_FEM) of D. Wan et al. [20]. (b) Bénard convection problem. (c) Case of migration of thermo-capillary droplets and the comparison of the time history with the reference solutions (Ref.) of M. Hopp-Hirschler et al. [5] and Tong et al. [11].

In Fig. 1 (a)-(b) results are compared with the literature [1, 19] and SPH resolutions (Δx). It is shown the isothermal streamlines and contour lines on the velocity and temperature fields of the particles. Likewise, Fig. 1 (a) shows the velocity and temperature profiles on the vertical line at $y = 0.5$ for the square cavity.

The vertical velocity and temperature profiles along the x-axis at and $y = 0.5$ are shown in Fig. 1 (a) for Ra=10^4. Profiles are almost independent of the resolution and in good agreement with the reference solution (T_FEM and Vel_FEM) of D. Wan et al. [20]. Even with higher resolution it is observed a tiny deviation from the available literature [20, 21].

For the cases with the thermo-capillary flow at the interface with a droplet into the square cavity (1x1) in Fig. 1 (c). The thermo-capillary dimensionless numbers for calibration are the Reynolds number ($\mathrm{Re} = \rho \mathrm{R}\mathrm{U_R}/\mu = 0.72$), Marangoni number ($\mathrm{Ma} = \rho c_p R\mathrm{U_R}/\kappa = 0.72$) and, Capillary number ($\mathrm{Ca} = \rho\mu\mathrm{U_R}/\sigma_0 = 0.0576$), where $\mathrm{U_R} = \sigma_T\Delta T\mathrm{R}/\mu$ is characteristic velocity, $\mathrm{R} = 0.5$ is the droplet radius, $\sigma_0 = 2.5$, $\sigma_T = 0.576$, $c_p = 1.0$, $T_0 = 0.5$, $\mu = 10^{-2}$, and $\rho = 500$ is the density of the fluid surrounding with the ration of viscosity and density between liquid and droplet equal to $\mu/\mu_\mathrm{R} = \rho/\rho_\mathrm{R} = 2$.

Figure 1 (c) displays the approach of the problem of migration of thermo-capillary droplets [4] for different Δx. Here, it is exposed the particle velocity field distribution and the time history of the dimensionless velocity of the droplet ($\mathrm{U}^* = \left|\mathbf{v}_R\right|/\mathrm{U_R}$) in comparison with the literature [5, 11]. The cases were validated with other classical computational models such as Finite elements (FEM) or Finite Differences (FDM) [12, 20], showing similar results, which illustrates an adequate 2D implementation of heat transfer and thermo-capillary with the proposed SPH methodology in Figure 1.

Table 1 shows that the average Nusselt number ($\mathrm{Nu_{Av.}} = 1/L\int \mathrm{Nu}(y)\mathrm{dy}$) obtained by present work, FDM [22], FEM [20], DSC [20] and K .Szewc et al. 2011 [23] has similar tendencies for the example of natural convection in a square cavity. In addition, Fig. 3 also presents the local Nusselt number ($\mathrm{Nu}(y) = \left|\partial T/\partial x\right|_{y\in\mathrm{wall}}$)

along the cold wall at two different Ra. It can be seen that the Nusselt number profiles obtained are good agreement between results. Furthermore, the increase in Nu along the vertical wall indicates that the convective heat transfer between the wall and the fluid is increased with increasing Rayleigh number.

	$\mathrm{Nu}_{\mathrm{Av.}}$						
Ra	1/50	1/100	1/200	FDM [22]	FEM [20]	DSC [20]	SPH(Szewc [23])
10^3	1.075	1.099	1.127	1.118	1.117	1.073	1.04
10^4	2.247	2.248	2.266	2.243	2.254	2.155	2.18
10^5	4.346	4.518	4.481	4.519	4.598	4.358	4.34
10^6	8.283	8.734	9.207	8.800	8.976	8.632	–

Table 1. Comparison of the average Nusselt number ($\mathrm{Nu}_{\mathrm{Av.}}$) obtained at different Rayleigh numbers (Ra) for the steady-state solution.

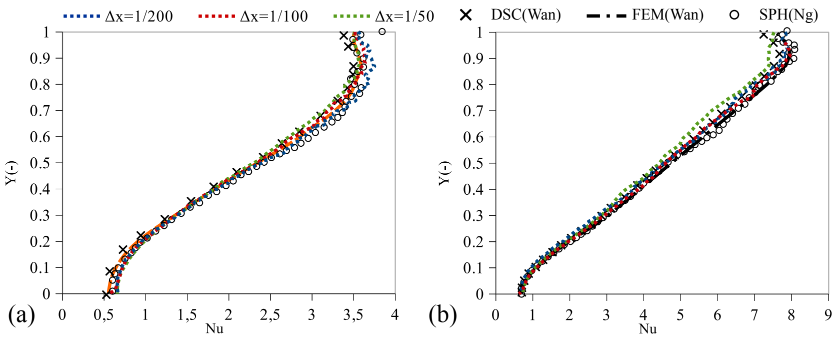

Figure 2. The local Nusselt number distribution along the cold wall for: (a) Ra=10^4. (b) Ra=10^5. References data were obtained by D. Wan et al. [20] and K. Ng et al. [21].

Results for the natural convection and thermo-capillarity are introduced using the 3D SPH approach as an extension for the 2D case. The distribution of the steady state in the cubic cavity (1x1x1) from the particles' velocity field, streamlines distribution, and particles temperature field is introduced in Fig. 3 for Ra numbers equals to 10^4 (Fig. 3 (a)) and 10^6 (Fig. 3 (a)). In this way, the results expose the movement of the particles according to the natural convection drive flow between the hot wall (left) and the cold wall (right). The solution approximation for the cubic cavity has the same tendency as a square cavity (Fig. 3).

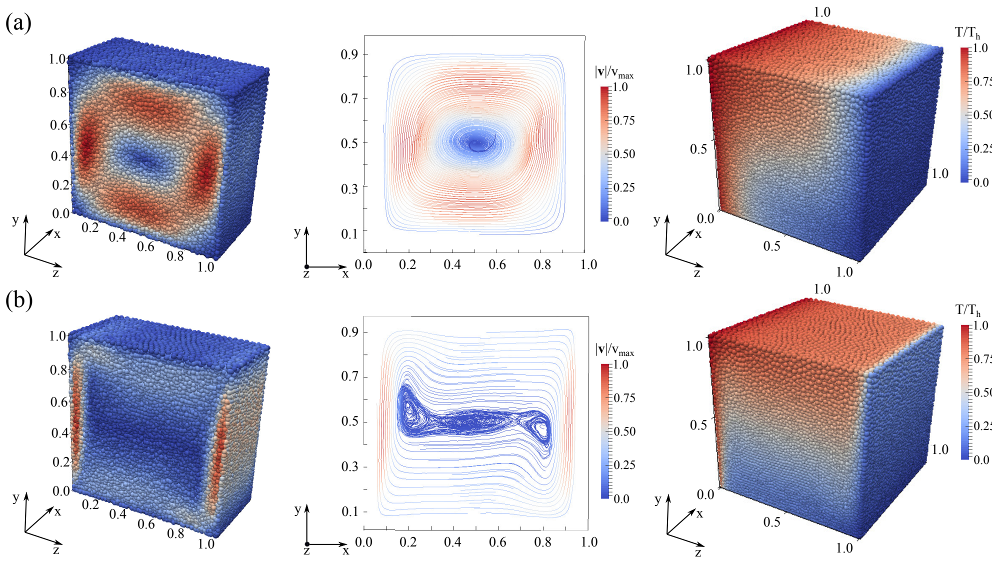

Figure 3. The particles' velocity field and streamlines spread in mid-plane, and the temperature distribution of the cubic cavity. The resulting distribution of particles: (a) Ra= 10^4; (b) Ra= 10^6.

In this part, examples of heat transfer and thermo-capillary migration are implemented as a studio case in a 3D configuration in Fig. 4, resembling cavity systems with considerable thermal influence on the fluid under hydrodynamic conditions. Thus, for the case of Fig. 4 (a) with a parallelepiped cavity (1x5x1), it is observed that the temperature change, generating a dense region in the bottom layer, rises in plumes that form the cells of Bérnad [2, 12], where it can observe the effects both on the temperature distribution for the two cases with Ra and its effects on the generation of vortices (streamlines) and the velocity field.

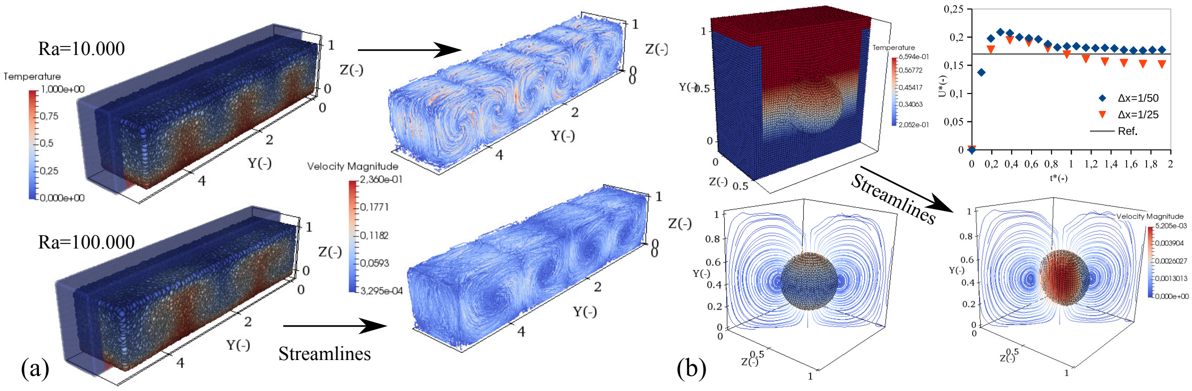

Figure 4. (a) Bénard convection problem in a parallelepiped cavity. (b) Case of migration of thermocapillary droplets in a cubic cavity and the comparison of the time history with the reference solutions (Ref.) of M. Hopp-Hirschler et al. [5] and Ma et al. [12].

Similarly, the case of thermo-capillary droplet migration inside a cubic cavity (1x1x1) shows the effects of the temperature gradient on velocities and flow lines over the 3D domains, analogous to the results reported in the literature [5, 12]. For the two examples, both natural convection and thermo-capillary, results are similar to the 2D cases in Fig. 1 (b) and (c). These examples in the formation of droplets expose the capacity and the great potential of the SPH methodology and the proposed simulation algorithm for the study of more refined cases of formation and behavior of emulsions and heat exchanges with interface [24, 25].

5 Conclusions

SPH approach for 2D and 3D proposed in this work explored cases with heat exchange and flow driven by surface tension (capillarity) and temperature gradients. Buoyancy-controlled flow is investigated for different Rayleigh numbers and compared with reference solutions for the case of natural convection. Therefore, the validation of this proposed model shows promising results and convergence with the literature. Finally, the migration of thermo-capillary droplets in a temperature field with a temperature-dependent surface tension coefficient is studied. The SPH thermo-capillarity shows an adequate approximation. Finally, the SPH methodology for coupling heat transfer, convection, and capillarity correctly model the cases treated in this work.

Acknowledgements. The authors acknowledge the São Paulo Research Foundation (FAPESP) (Grant no. 21/05931-9, 17/50343-2, and 13/08293-7) and EPSRC New Investigator Award (Grant no. EP/T000775/1) for the financial support of this research.

Authorship statement. The authors confirm contribution to the paper as follows: study conception and design: E. A. Patiño-Nariño, M. R. Gongora-Rubio; data collection: E. A. Patiño-Nariño; analysis and interpretation of results: E. A. Patiño-Nariño, A. F. Galvis, R. Pavanello, M. R. Gongora-Rubio; draft manuscript preparation: E. A. Patiño-Nariño, A. F. Galvis. All authors reviewed the results and approved the final version of the manuscript.

References

[1] A. M. Aly. Modeling of multi-phase flows and natural convection in a square cavity using an incompressible smoothed particle hydrodynamics. *International Journal of Numerical Methods for Heat & Fluid Flow*, vol. 25, n. 3, pp. 513–533, 2015.

[2] H. Su, X. Feng, and J. Zhao. Penalty decoupled iterative methods for the stationary natural convection equations with different Rayleigh numbers. *Applied Numerical Mathematics*, vol. 163, n. 11701493, pp. 270–291, 2021.

[3] E. A. Patino-Narino, H. S. Idagawa, de D. S. Lara, R. Savu, S. A. Moshkalev, and L. O. S. Ferreira. Smoothed particle hydrodynamics simulation: a tool for accurate characterization of microfluidic devices. *Journal of Engineering Mathematics*, vol. 115, n. 1, pp. 183–205, 2019.

[4] C. Meier, S. L. Fuchs, A. J. Hart, and W. A. Wall. A novel smoothed particle hydrodynamics formulation for thermo-capillary phase change problems with focus on metal additive manufacturing melt pool modeling. *Computer Methods in Applied Mechanics and Engineering*, vol. 381, pp. 113812, 2021.

[5] M. Hopp-Hirschler, M. S. Shadloo, and U. Nieken. A Smoothed Particle Hydrodynamics approach for thermo-capillary flows. *Computers and Fluids*, vol. 176, pp. 1–19, 2018.

[6] E. A. Patiño-Nariño, A. F. Galvis, P. Sollero, R. Pavanello, and S. A. Moshkalev. A consistent multiphase SPH approximation for bubble rising with moderate Reynolds numbers. *Engineering Analysis with Boundary Elements*, vol. 105, pp. 1–19, 2019.

[7] S. Adami, X. Hu, and N. Adams. A new surface-tension formulation for multi-phase SPH using a reproducing divergence approximation. *Journal of Computational Physics*, vol. 229, n. 13, pp. 5011–5021, 2010.

[8] G. K. Batchelor and A. D. Young. *An Introduction to Fluid Mechanics*, volume 35. Cambridge University Press, Cambridge, 1968.

[9] J. U. Brackbill, D. B. Kothe, and C. Zemach. A continuum method for modeling surface tension. *Journal of Computational Physics*, vol. 100, n. 2, pp. 335–354, 1992.

[10] A. Zhang, P. Sun, and F. Ming. An SPH modeling of bubble rising and coalescing in three dimensions. *Computer Methods in Applied Mechanics and Engineering*, vol. 294, n. 145, pp. 189–209, 2015.

[11] M. Tong and D. J. Browne. An incompressible multi-phase smoothed particle hydrodynamics (SPH) method for modelling thermocapillary flow. *International Journal of Heat and Mass Transfer*, vol. 73, pp. 284–292, 2014.

[12] C. Ma and D. Bothe. Direct numerical simulation of thermocapillary flow based on the Volume of Fluid method. *International Journal of Multiphase Flow*, vol. 37, n. 9, pp. 1045–1058, 2011.

[13] C. Geuzaine and J. F. Remacle. Gmsh: A 3-D finite element mesh generator with built-in pre- and post-processing facilities. *International Journal for Numerical Methods in Engineering*, vol. 79, n. 11, pp. 1309–1331, 2009.

[14] S. Adami, X. Y. Hu, and N. Adams. A generalized wall boundary condition for smoothed particle hydrodynamics. *Journal of Computational Physics*, vol. 231, n. 21, pp. 7057–7075, 2012.

[15] K. Moreland. The ParaView Tutorial. *Sandia National Laboratories*, pp. 129, 2011.

[16] E. A. Patiño-Nariño, A. F. Galvis, R. Pavanello, and S. A. Moshkalev. Numerical study of single bubble rising dynamics for the variability of moderate Reynolds and sidewalls influence: A bi-phase SPH approach. *Engineering Analysis with Boundary Elements*, vol. 129, n. April, pp. 1–26, 2021.

[17] A. Smolianski, H. Haario, and P. Luukka. Numerical study of dynamics of single bubbles and bubble swarms. *Applied Mathematical Modelling*, vol. 32, n. 5, pp. 641–659, 2008.

[18] L. Li, H. Su, and X. Feng. Recovery-Based Error Estimator for Natural Convection Equations Based on Defect-Correction Methods. *Entropy*, vol. 24, n. 2, 2022.

[19] A. M. Aly and Z. A. Raizah. Double-diffusive natural convection in an enclosure filled with nanofluid using ISPH method. *Alexandria Engineering Journal*, vol. 55, n. 4, pp. 3037–3052, 2016.

[20] D. C. Wan, B. S. Patnaik, and G. W. Wei. A new benchmark quality solution for the buoyancy-driven cavity by discrete singular convolution. *Numerical Heat Transfer, Part B: Fundamentals*, vol. 40, n. 3, pp. 199–228, 2001.

[21] K. Ng, Y. Ng, T. Sheu, and A. Alexiadis. Assessment of Smoothed Particle Hydrodynamics (SPH) models for predicting wall heat transfer rate at complex boundary. *Engineering Analysis with Boundary Elements*, vol. 111, n. November 2019, pp. 195–205, 2020.

[22] G. de Vahl Davis. Natural convection of air in a square cavity: a bench mark numerical solution. vol. 3, n. (Report 1982-FMT-2), pp. 249–264, 1982.

[23] K. Szewc, J. Pozorski, and A. Tanire. Modeling of natural convection with Smoothed Particle Hydrodynamics: Non-Boussinesq formulation. *International Journal of Heat and Mass Transfer*, vol. 54, n. 23-24, pp. 4807–4816, 2011.

[24] M. Wörner. Numerical modeling of multiphase flows in microfluidics and micro process engineering: A review of methods and applications. *Microfluidics and Nanofluidics*, vol. 12, n. 6, pp. 841–886, 2012.

[25] P. Pattanayak, S. Kumar, S. Monica, G. Sukriti, and V. Bhupinder. Microfluidic chips : recent advances , critical strategies in design , applications and future perspectives. *Microfluidics and Nanofluidics*, pp. 1–28, 2021.

[26] D. Mamalis, V. Koutsos, and K. Sefiane. Bubble rise in a non-isothermal self-rewetting fluid and the role of thermocapillarity. *International Journal of Thermal Sciences*, vol. 117, pp. 146–162, 2017.